American Mineralogist, Volume 100, pages 945–950, 2015

Complex IR spectra of OH^- groups in silicate glasses: Implications for the use of the 4500 cm^{-1} IR peak as a marker of OH^- groups concentration

Charles Le Losq[1,*], George D. Cody[1] and Bjorn O. Mysen[1]

[1]Geophysical Laboratory, Carnegie Institution of Washington, 5251 Broad Branch Road NW, Washington, D.C. 20015, U.S.A.

Abstract

Previous studies of hydrous glasses and melts with infrared spectroscopy have led to the conclusion that the IR combination peaks near 4500 and 5200 cm^{-1} reflect the existence of OH^- (hydroxyl) groups and H_2O_{mol} water molecules in those materials. Here, we show that the glass chemical composition can impact profoundly the intensities and frequencies of the fundamental O-H stretching signal and, therefore, potentially those of the 4500 and 5200 cm^{-1} combination peaks. In alkali silicate glasses, compositional effects can give rise to peaks assigned to fundamental O-H stretching at frequencies as low as 2300 cm^{-1}. This expanded range of Raman intensity assigned to O-H stretch is increasingly important as the ionic radius of the alkali metal increases. As a result, the combination of the fundamental O-H stretch in OH^- groups with the Si-O-H stretch located near 910 cm^{-1} gives rise to a complex combination signal that can extend to frequencies much lower than 4200 cm^{-1}. This combination signal then becomes unresolvable from the high-frequency limb of the band assigned to fundamental O-H stretch vibration in the infrared spectra. It follows that, when O-H stretch signals from OH^- groups extend to below 3000 cm^{-1}, the 4500 cm^{-1} peak does not represent the total OH^- signal. Under such circumstances, this infrared peak may not be a good proxy for determining the concentration of OH^- hydroxyl groups for glassy silicate materials.

Keywords: Water speciation, FTIR spectroscopy, O-H stretch signal, silicate glasses

Introduction

Water dramatically affects the physical properties of silicate melts and glasses (see the review by Mysen and Richet 2005), and, as a result, is of key importance in both industrial and geologic processes. An important feature of water dissolved in glassy and molten silicate materials is that it exists both as molecules (H_2O_{mol}) and as hydroxyl groups (OH^-) bonded to the silicate network. It has often been stated that those two different species give rise to IR combination peaks at ~5200 and ~4500 cm^{-1}, respectively (Davis and Tomozawa 1996; Efimov and Pogareva 2006; Malfait 2009; Scholtze 1960; Stolper 1982). The OH^- groups are bonded to the tetrahedral network of silicate glasses and melts, forming Si-OH and Al-OH bonds by breakage of bridging oxygen bonds (Si-O-Si, Al-O-Al, and Si-O-Al) (see for instance Moulson and Roberts 1961; Scholtze 1960; Stolen and Walrafen 1976; Stolper 1982). This solution mechanism results in depolymerization of the silicate network (see for instance the study of Mysen and Cody 2005). In contrast, water dissolved in the form of H_2O_{mol} species does not change melt polymerization. As a result, the dissolution of water as OH^- groups or as H_2O_{mol} species has different effects on the polymerization and hence properties of hydrous silicate amorphous materials. These differences are reflected in transport properties of hydrous melts, glass transition temperature (see for instance Deubener et al. 2003), solidus temperatures, melt/mineral phase equilibria, and element partitioning (see for a review Mysen and Richet 2005).

The water speciation, in terms of H_2O_{mol} species and OH^- groups, varies with total water concentration and temperature (Behrens and Yamashita 2008; Nowak and Behrens 1995; Stolper 1982). It also depends on composition (Deubener et al. 2003; Moretti et al. 2014). However, it is not known how temperature effects vary with bulk composition, and how bulk compositional variables govern solution mechanisms and solubility.

FTIR spectroscopy may be used to examine such effects by using the combination peaks often located near 4500 and 5200 cm^{-1} in the spectra. However, as a first step, it is necessary to ascertain exactly what governs the frequency and integrated intensity of the 4500 and 5200 cm^{-1} combination peaks in the IR spectra of hydrous silicate glasses (and melts). An example of this is the recent work of Malfait (2009) who concluded that the 4500 cm^{-1} IR peak is formed by the combination of the fundamental O-H stretching mode at ~3600 cm^{-1} with the Si-O-H, and presumed Al-O-H, stretching vibrational mode. The Al-O-H vibrational mode can occur near 800 cm^{-1}, whereas the Si-O-H is near 920 cm^{-1}. Combined with the fundamental O-H stretching mode at 3600 cm^{-1} in simple aluminosilicate glasses, the exact frequency of the 4500 cm^{-1} would be somewhat correlated, therefore, with the Al/Si of the glass. Concerning the 5200 cm^{-1} peak, it is attributed to arise from the combination of the 3600 cm^{-1} stretching and 1630 cm^{-1} bending modes of H_2O_{mol} species (Scholtze 1960; Stolper 1982).

The infrared signal assigned to O-H stretch in OH^- and H_2O_{mol} species, usually characterized by an asymmetric band centered near 3600 cm^{-1}, can have a complex shape in some silicate glasses, where broad bands extend into the 2000–3000 cm^{-1}

* E-mail: clelosq@carnegiescience.edu

0003-004X/15/0004–945$05.00/DOI: http://dx.doi.org/10.2138/am-2015-5076

frequency range (see for instance data on sodium silicate glasses of Uchino et al. 1991; Zotov and Keppler 1998). If those bands are from OH^- groups, then their combination with the Si-O-H stretch mode located near 910 cm^{-1} (Zotov and Keppler 1998) will give OH^- combination signals at frequencies significantly lower than 4500 cm^{-1}. However, if the low-frequency signals are from O-H stretch in H_2O_{mol} species, their combination with the H_2O_{mol} bending mode near 1630 cm^{-1} will result in signals in the range of the OH^- combination peak. In both cases, using the intensities of the 4500 and 5200 cm^{-1} peaks would be not appropriate to determine the [OH^-] and [H_2O_{mol}] concentration in the glass. To evaluate impacts of such effect and their consequence for the determination of [OH^-] and [H_2O_{mol}], we studied alkali (Li, Na, K) silicate glasses containing different amount of dissolved water by using FTIR and Raman spectroscopies.

Experimental methods

Anhydrous KS4 ($K_2Si_4O_9$), NS4 ($Na_2Si_4O_9$), and LS4 ($Li_2Si_4O_9$) glasses were synthetized by mixing pure anhydrous SiO_2, K_2CO_3, Na_2CO_3, and Li_2CO_3 powders and grinding them under ethanol for about 1 h. The powders were placed in a Pt crucible and heated at about 1.5°/min until reaching 1000 °C before bringing the samples to complete melting. Melting was accomplished near 1200 °C for the KS4 composition, 1400 °C for the NS4 composition, and 1600 °C for the LS4 composition, in agreement with their respective liquidus temperature (Eppler 1963; Schairer and Bowen 1955, 1956). Melts were quenched to glass by placing the bottom of the crucible in liquid H_2O. The resulting starting materials were stored at 110 °C to avoid reaction with atmospheric water, an effect particularly critical for the KS4 glass (Schairer and Bowen 1955). Chemical analysis of the starting glasses, shown in Table 1, were obtained by using a JEOL FE-SEM equipped with an energy-dispersive spectrometer. Measurements were performed on 25 × 25 µm areas with a 15 kV and 1.04 nA current. Lithium was quantified by difference.

Hydrous glasses were synthesized by melting the starting glasses together with known amounts of H_2O in a piston-cylinder apparatus (Boyd and England 1960). To this end, glasses were first crushed to powder in ethanol, and then heat-treated at 400 °C for 1 h to ensure complete removal of the ethanol. Then, glass powder and liquid H_2O were added in ~10 mm long, 5 mm diameter platinum capsules, which were welded shut and placed in ¾-inch diameter furnace assemblies, based on the design of Kushiro (1976). The products were then subjected to the desired pressure (1.5 GPa) and temperature (1450 °C for NS4, 1550 °C for KS4, and 1650 °C for LS4) for 90 min. Temperatures were measured with type S thermocouples with no correction for pressure on their *emf*. Such pressure effects may be as much as 10 °C (Mao et al. 1971). Pressure was calibrated against the melting point of NaCl and the calcite-aragonite transformation (Bohlen 1984). Estimated uncertainties are ~10 °C and ~0.1 GPa, respectively.

Table 1. Chemical composition of LS4, NS4, and KS4 anhydrous glasses

		SiO_2	Li_2O[a]	Na_2O	K_2O
LS4	nom. mol%	80.00	20.00	0.00	0.00
	nom. wt%	88.94	11.08	0.00	0.00
	meas. wt%	88.77(94)	11.23(75)	n.a.	n.a.
NS4	nom. mol%	80.0	20.0	0.00	0.00
	nom. wt%	79.50	0.00	20.50	0.00
	meas. wt%	80.38(36)	n.a.	19.62(31)	n.a.
KS4	nom. mol%	80.0	20.0	0.0	0.0
	nom. wt%	71.84	0.00	0.00	28.16
	meas. wt%	71.16(49)	n.a.	n.a.	28.84(28)

Notes: nom. mol%, nom. wt%, and meas. wt% refer, respectively, to the nominal compositions in mol and wt%, and to the measured composition in wt%.
[a] Lithium has been determined by difference. Errors are given at the 1σ confidence interval.

Transmission infrared spectra were recorded using a Jasco IMV-4000 multichannel infrared spectrometer with a 10× objective, an MCT detector and the standard light source, a 100 µm aperture, and 1000 acquisitions. The hydrous glasses were double-polished to a thickness in the 20–110 µm range by using oil to avoid any reaction of their surface with water. For KS4 composition glasses, two sets of samples were used. One was ~20 µm thick and was used for recording the 3600 cm^{-1} O-H stretching band. However, those ~20 µm samples were to thin for acquisition of combination signals. Consequently, another thicker set of samples (~100 µm) were prepared for this purpose. The glass samples were placed on BaF_2 windows during measurements. After each spectrum, the sample was moved aside and a background spectrum was recorded at the same spot. Division of sample spectra by background spectra gave the final absorbance spectra, which were normalized to samples thicknesses.

Raman spectra were recorded using a Jasco NRS3100 spectrometer, equipped with a holographic notch filter, a single monochromator, and a 1024 × 128 Andor DV401-F1 CCD Peltier-cooled at –71 °C. A Coherent solid laser line of 490 nm was used to excite samples, with a power of ~44 mW on the sample. The laser beam was focused through a 50× Olympus lens. Measurements were done with a 1200 grooves/mm grating. Frequency accuracy of the Raman spectrometer was checked by using the 520.7 cm^{-1} Raman peak of pure silicon. All spectra are unpolarized. After acquisition, a baseline constrained in the spectral portions devoid of signal near 2000 and 3900 cm^{-1} was subtracted from the spectra. The intensities of baseline-subtracted spectra were normalized to their total spectral area (calculated between 250 and 3900 cm^{-1}). Further details about spectra processing are available in Le Losq et al. (2015).

Total water concentration of glasses was estimated by using the FTIR and Raman spectra. Absorption coefficients for the 4500 and 5200 cm^{-1} IR peaks in NS4 glasses are available in the literature. We used the protocol of Yamashita et al. (2008) together with their absorption coefficients, which were derived by using total water concentrations determined independently with Karl-Fisher titration. Because of that and despite the fact that the present study will discuss the use of the 4500 cm^{-1} IR peak for inferring [OH^-] abundance, the FTIR-based [OH^-] + [H_2O_{mol}] sum is not affected by possible error in the assignments and attributions of the IR absorption peaks. As IR absorption coefficients are not available for KS4 and LS4 glasses, Raman spectroscopy was used to estimate the water concentration of these glasses. A protocol similar to that described in Le Losq et al. (2012) was used. The variations of the areas of the Raman signals assigned to O-H stretching, located between 2000 and 4000 cm^{-1}, was calibrated with the FTIR-based total water concentrations of the same NS4 glasses. This calibration was then used with the other LS4 and KS4 glass series to determine their water concentration. More details are available in Le Losq et al. (2015). Table 2 reports the measured water concentrations of the glasses.

Results

In the FTIR spectra of hydrous alkali silicate glasses, strong peaks at ~1630 (ν_B H-O-H), ~2350 (A in Fig. 1), ~2800 (B in Fig. 1), and ~3570 cm^{-1} (C in Fig. 1) are observed. The IR spectra of hydrous NS4 glasses are similar to those previously published

Table 2. Water concentration in mol% and wt% of glasses

			wt% H_2O		FTIR absorption, cm^{-1}		
Glass	nom. mol% H_2O	nom. wt% H_2O	FTIR	Raman	I_A	I_B	I_C
LS4	3.28	1.12	–	1.05(30)	38.6	49.5	76.1
	9.40	3.35	–	3.61(30)	98.3	152.8	277.2
	17.64	6.67	–	7.15(30)	190.0	316.3	603.7
NS4	3.28	1.00	1.21(12)	1.05(30)	96.4	100.0	37.1
	9.40	3.00	2.89(18)	3.02(30)	238.6	264.3	124.8
	17.64	6.00	6.00(29)	5.96(30)	500.5	604.2	383.7
KS4	3.28	0.90		1.10(30)	172.4	166.0	31.8
	9.40	2.71	–	2.78(30)	344.6	345.4	65.1
	17.64	5.44	–	4.85(30)	702.1	729.9	138.2

Notes: Nom. = nominal water concentration. I_A, I_B, and I_C FTIR absorbance intensities correspond to those observed on Figure 1 for peaks A, B, and C (as this is for indicative purpose, no error are indicated). Errors are given at the 2σ confidence interval.

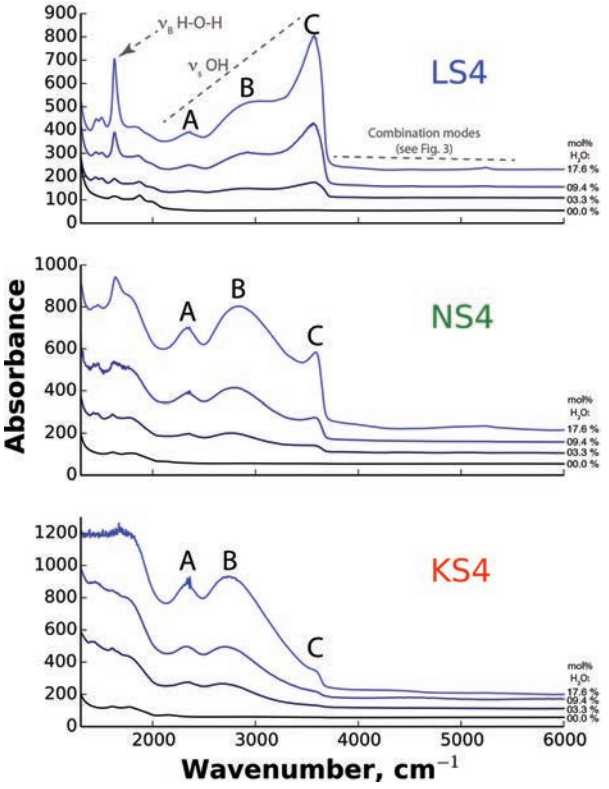

Figure 1. FTIR spectra of LS4 (**top**), NS4 (**middle**), and KS4 (**bottom**) glasses with 0.0, 3.3, 9.4, and 17.6 nom. mol% water (from bottom to top in the figures, respectively). A, B, and C are visual markers for the three observed peaks attributed to the O-H stretch (ν_s O-H) in H_2O_{mol} and OH^- groups. The peak at 1630 cm^{-1} arises from the bending of H_2O_{mol} (ν_B H-O-H). Signal below 1300 cm^{-1} is at saturation and therefore not shown here. Spectra are offset of 5 absorbance units for clarity. (Color online.)

for NS4 hydrous compositions (e. g., Uchino et al. 1991; Zotov and Keppler 1998). Spectra of hydrous KS4 and LS4 glasses have not been reported in the literature to our knowledge.

The three peaks (A, B, and C) in the 2000–4000 cm^{-1} portion of FTIR spectra are attributed to stretching of O-H bonds in H_2O_{mol} and OH^- groups. The 1630 cm^{-1} peak is assigned to the bending vibrational mode of H_2O_{mol} species (Bartholomew et al. 1980; Scholtze 1960; Uchino et al. 1991; Wu 1980; Zotov and Keppler 1998). The other small peaks located at frequencies below 2000 cm^{-1} probably arise from overtones of the vibrational modes of the glass silicate network (see the study of Efimov and Pogareva 2006 for instance) and are neglected because of their minor importance regarding the topic of this study. Above 3800 cm^{-1}, peaks from the combination modes are present but not visible at the scale of Figure 1. They will be discussed in detail latter.

In the IR spectra of all glasses, the peaks A and B are broad, whereas the peak C is considerably sharper. Absorbance values of those peaks are reported in Table 2. At given water concentration, the absorbance intensities vary strongly as a function of the ionic radius of the alkali metal (Fig. 1). The absorbance intensities of peaks A and B increase strongly with increasing ionic radius of alkali, whereas that of peak C decreases. In a given composition, increasing water content results in a general absorbance increase of all contributions, but the absorbance of the ~3600 cm^{-1} contribution increases slightly more rapidly than the others (Table 2 and Fig. 1).

The three peaks in the infrared spectra, A, B, and C, are also visible in Raman spectra of the same glasses (Fig. 2). As already emphasized by FTIR data (Fig. 1), the comparison of the spectra of the silicate glasses containing 17.6 mol% H_2O highlights that with increasing the ionic radius of the alkali, peaks A and B grow at the expense of the peak C. For comparison purposes, the Raman spectrum of a pure SiO_2 glass with 20 mol% H_2O is also reported in Figure 2. In this latter spectrum, the signal intensity below 3000 cm^{-1} is negligible compared with the intensity between 3000 and 4000 cm^{-1}. The two peaks located near 3595 and 3650 cm^{-1} can be attributed to O-H stretching from OH^- groups in different environments (the 3595 cm^{-1} peak is only observed in H_2O-rich silica glasses), but their attribution remains unclear and is subjected to speculation (see for instance the studies of Davis and Tomozawa 1996; Efimov and Pogareva 2006; Holtz et al. 1996; Mysen and Virgo 1986).

The shape of the peaks near 4500 and 5200 cm^{-1} in the IR spectra also varies significantly with the glass composition at given total water content (Fig. 3). In IR spectra of the LS4 glasses, two asymmetric peaks are observed at ~4520 and ~5240 cm^{-1}. Their intensities increase with increasing water concentration, but in different ways. The ~4520 cm^{-1} peak is more intense than the ~5240 cm^{-1} peak in the IR spectrum of the LS4 + 3.3 mol% H_2O glass (Figs. 3 and 4). In contrast, at 17.6 mol% H_2O, the ~5240 cm^{-1} peak is more intense than the ~4520 cm^{-1}. Therefore, the intensity of the ~4520 cm^{-1} peak increases less and less with water addition, whereas that of the ~5240 cm^{-1} peak shows an

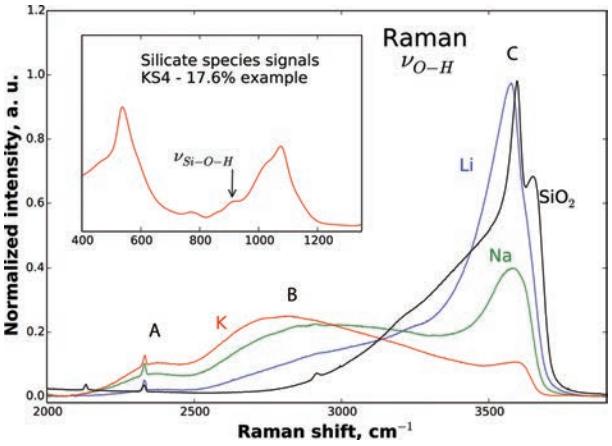

Figure 2. Raman O-H stretching signal in the KS4, NS4, and LS4 glasses with 17.6 nom. mol% H_2O. For comparison, the peak assigned to O-H stretch in a SiO_2 glass with 20 mol% H_2O is also shown (made at 1.5 GPa, 1650 °C). A, B, and C are visual markers for the three observed peaks (see also Fig. 1). Small sharp peaks near 2330 cm^{-1} arise from the N_2 atmospheric signal. Insert: signals from the Si-O-Si bending (the 500 cm^{-1} band) and the Si-O stretching modes (the 1100 cm^{-1} band) of the KS4 + 17.6 mol% H_2O are shown (see Le Losq et al. 2014; Mysen 1990; Mysen and Cody 2005; Mysen et al. 1982 for more details and attributions for silicate species); the signal from the Si-O-H stretch may give rise to the peak near 910 cm^{-1} that is perfectly visible on this spectrum (Malfait 2009; Spiekermann et al. 2012; Zotov and Keppler 1998). (Color online.)

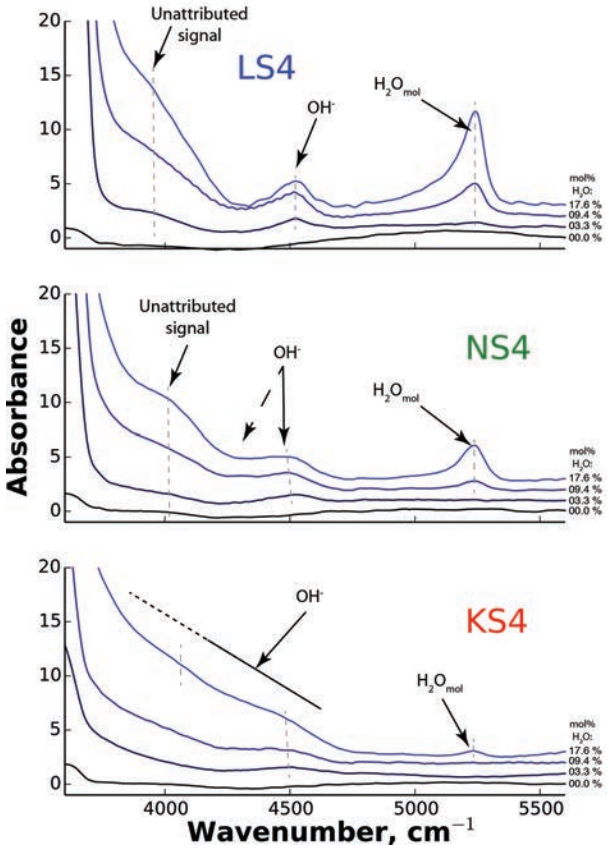

FIGURE 3. Details of the 3800–5600 cm^{-1} region of the FTIR spectra of KS4, NS4, and LS4 glasses. From bottom to top in the figures: 0.0, 3.3, 9.4, 17.6 nom. mol% H_2O. Spectra are offset of 1 absorbance unit for clarity. The dotted lines indicate the presence of peaks in the spectra (see text). (Color online.)

opposite trend (Fig. 4). If these two IR peaks are attributed to OH^- (4520 cm^{-1}) and H_2O_{mol} (5240 cm^{-1}) species, as has commonly been the case (see Introduction), their intensity variations are consistent with a decrease of the OH^-/H_2O_{mol} ratio with increasing water concentration in LS4 glass. In addition to those two peaks, a small and broad peak near 4000 cm^{-1} is visible. This peak is well separated from the ~4520 cm^{-1} peak (Fig. 3, LS4 spectra). Its intensity increases with water concentration, but is also affected by the high-frequency tail of the 3600 cm^{-1} peak. Indeed, this tail shifts toward high frequency and probably varies in intensity with increasing water concentration (Fig. 3). This topological evolution probably affects the shape of the peak located near 4000 cm^{-1}. The origin of the latter is unresolved but may involve unidentified combination modes of both H_2O_{mol} and OH^- species (see the discussion of Stolper 1982 and also Davis and Tomozawa 1996; Efimov and Pogareva 2006).

The three peaks near 4000, 4520, and 5236 cm^{-1} also are observed in the IR spectra of NS4 hydrous glasses. Their intensities vary with water concentration in a way similar to that observed in the LS4 spectra (Figs. 3 and 4). However, the separation of the ~4000 and ~4520 cm^{-1} peaks is less pronounced in NS4 spectra than in LS4 spectra (Fig. 3). It becomes even less pronounced in the KS4 spectra, in which the peaks in the 3900–4700 cm^{-1} range are poorly defined (Fig. 3). In the KS4 + 3.3 mol% H_2O spectrum, a small peak at ~4510 cm^{-1} is observed, and there is no peak near 5200 cm^{-1}. No peak is observed near 4000 cm^{-1}, but the high-frequency end of the 3600 cm^{-1} O-H stretch band affects the intensity of the spectrum in the 3800–4200 portion of spectra (Fig. 3). In the KS4 + 9.4 mol% H_2O glass spectrum, the ~4510 cm^{-1} peak is barely visible. The IR absorbance between 3800 and 4800 cm^{-1} shows a global, nearly linear, decay. There is no intensity near 5200 cm^{-1} in this spectrum. At 17.6 mol% H_2O, the ~4510 cm^{-1} contribution is very broad and preceded by another broad small peak centered near 4050 cm^{-1}. Finally, a small symmetric peak is present at ~5230 cm^{-1} in the spectrum

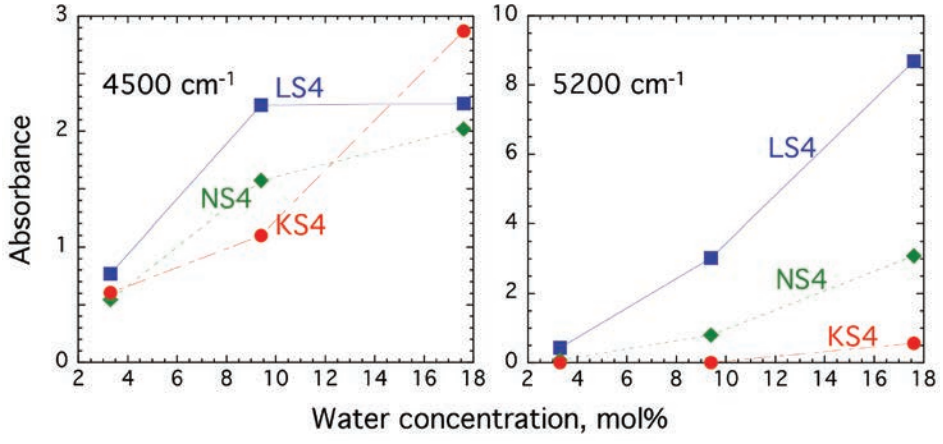

FIGURE 4. Absorbance of the peaks located at ~4500 and ~5200 cm^{-1}, observed on the spectra of hydrous glasses presented in Figure 3, reported as a function of the nominal water content of glasses. Absorbance was measured at the maximum intensity of peaks. Please note that those values were measured on spectra for which no background subtraction was applied, so that those values cannot be used to retrieve the water concentration of the glasses. Lines are guides for the eyes. (Color online.)

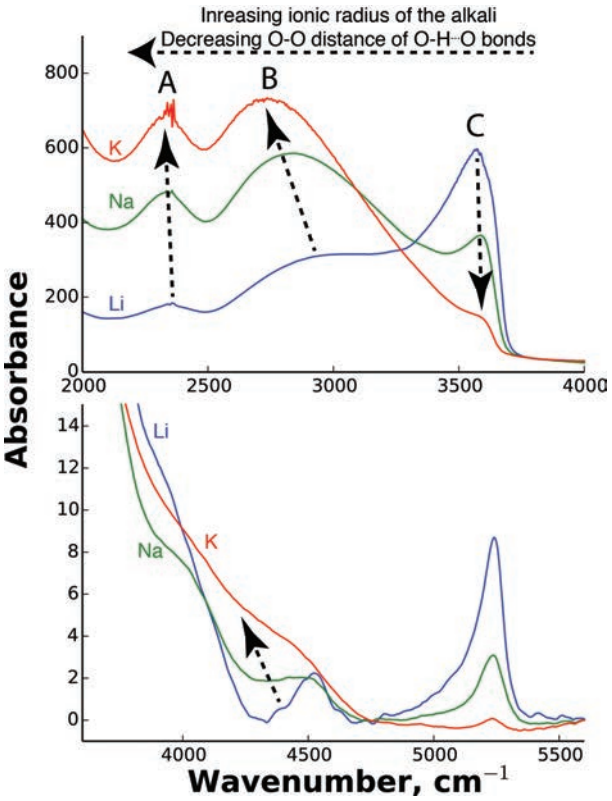

FIGURE 5. (**top**) 2000–4000 cm^{-1} portion of spectra of 17.6 mol% H_2O KS4, NS4, and LS4 glasses, the A, B, and C marker correspond to those on Figure 1; (**bottom**) 3800–5600 cm^{-1} region of same spectra. The arrows are used as visual marker for highlighting the effects produced by an increase of the ionic radius of the alkali in the glasses (see text). (Color online.)

of this water-rich composition.

The absence of the ~5200 cm^{-1} peak in the IR spectra of the KS4 with 3.3 and 9.4 mol% H_2O and its low intensity in the spectrum of KS4 with 17.6 mol% H_2O (Figs. 3 and 4) indicate that essentially all the water is present as OH^- groups in KS4 compositions, in agreement with results from ^{1}H NMR spectroscopy (Le Losq et al. 2015). In addition, the IR results and previous ^{1}H NMR data (Le Losq et al. 2015) both indicate that, at fixed water concentration, the OH^-/H_2O_{mol} ratio increases strongly with increasing ionic radius of alkali in the order Li < Na < K (Fig. 3; Le Losq et al. 2015). However, despite their very high OH^-/H_2O_{mol} ratios, the KS4 hydrous glasses show the less resolved OH^- combination peaks in their IR spectra in comparison to the NS4 and LS4 compositions (Fig. 3). Interestingly, they also show the highest intensities in the 4000–4700 cm^{-1} portion of spectra (see comparison in Fig. 5).

DISCUSSION

Increasing the ionic radius of the alkali cation in hydrous silicate glasses, formed by quenching melts equilibrated at high temperature and pressure, produces in both the FTIR and Raman spectra a strong intensity increase of two peaks at frequencies below 3000 cm^{-1} and attributed to O-H stretch in H_2O_{mol} and OH^- groups (Figs. 1, 2, and 5). The exact frequency of the contribution B also decreases by ~100 cm^{-1} with increasing the alkali ionic radius (Figs. 2 and 5). Such effect probably arises from the modification of the inter-oxygen O-O distance around protons (e.g., the distance of O-H···O bonds) as a function of the ionic radius of the alkali. Indeed, from ^{1}H NMR spectroscopy of the same alkali silicate glasses, a decrease of the mean O-O distance around protons does occur with increasing the ionic radius of the alkali (Le Losq et al. 2015). This mean O-O distance is ~287 pm in LS4 glasses and ~255 pm in KS4 glasses (Le Losq et al. 2014). The frequency of the IR and Raman bands assigned to O-H stretching is related to the inter-oxygen O-O distance around protons (Nakamoto et al. 1955; Novak 1974; Wall and Hornig 1965). From the data compilation of Novak (1974), the mean O-O distances of ~287 and ~255 pm correspond to mean O-H stretch frequency of ~3500 and ~2300 cm^{-1}, respectively. These frequencies correspond to the main peaks C and A in the FTIR and Raman spectra of LS4 and KS4 glasses (Figs. 2 and 3). Therefore, FTIR and Raman data confirm that increasing the alkali ionic radius in hydrous binary silicate glasses promotes a decrease of O-O distances around protons.

An increase of the alkali ionic radius also results in a significant increase of the OH^-/H_2O_{mol} ratio, so that the hydrous KS4 glasses, for example, contain mostly OH^- groups, at least up to the maximum total water content of this study (17.6 mol % H_2O). Given that peaks A and B are well expressed in the KS4 glasses (Figs. 1, 2, 3, and 5), it appears that those two peaks arise from O-H stretch in OH^- groups. Therefore, their combination with the Si-O-H stretch vibrational mode located near 910 cm^{-1} (Fig. 2) must give a complex OH^- combination signal. This is indeed observed when superimposing the spectra of the 17.6 mol% glasses (Fig. 5, bottom). As the alkali ionic radius increases, the intensity of peaks A and B increase. As a result, the intensity between 4100 and 4400 cm^{-1} also increases (arrow in Fig. 5, bottom), and the signal between 4000 and 4700 cm^{-1} becomes less and less resolved. Consequently, the combination of the O-H fundamental stretch signals from OH^- groups with the signal assigned to Si-O-H stretching can result in a broad combination signal that extends from 4700 cm^{-1} down to at least 3800 cm^{-1}, and thus becomes mixed with the unattributed ~4000 cm^{-1} peak and with the high-frequency end of the O-H stretching band in the IR spectra (Fig. 5).

IMPLICATIONS

The IR combination signal of OH^- groups is often reported to be near 4500 cm^{-1} because most of the signals assigned to O-H stretch are located above 3000 cm^{-1} in many aluminosilicate glasses (Stolper 1982). However, the data reported here show that IR combination signals used to study the speciation of water in glasses and melts can be complex because of the strong dependence of the O-H stretch frequency on the O-O distances around protons, and hence, on the glass structure. In any study of hydrous silicate glasses, the strong dependence of the proton environment as a function of the type of metallic cation within the silicate network of glasses must be kept in mind, because this dependence affects the IR combination signals and therefore the accuracy of the determination of water speciation with IR spectroscopy. The combination peaks in IR spectra of alkali-rich or alkaline-earth rich natural compositions, such as alkali

phonolite and phono-trachyte for instance, may, therefore, be broadened as illustrated in the simple compositions used in this study. However, this is purely speculative at this time and has to be investigated. In all cases, we advise users to check the occurrence and importance of low-frequency (<3000 cm^{-1}) O-H stretching signals in glasses before using the 4500 and 5200 cm^{-1} combination peaks as proxies for [OH^-] or [H_2O_{mol}]. If those low-frequency O-H stretching signals are significant, any use of the combination peaks to determine [OH^-] or [H_2O_{mol}] is problematic.

Acknowledgments

We thank John Armstrong (GL-CIW) for his help with SEM analyses of the glasses. We also acknowledge Zoltan Zajacz, an anonymous reviewer and the associate editor Grant Henderson for their helpful comments that helped improving this manuscript. This research was partially supported by grants EAR1212754 and EAR1251931 to B.O.M. and the NASA Astrobiology Institute.

References cited

Bartholomew, R.F., Butler, B.L., Hoover, H.L., and Wu, C.K. (1980) Infrared spectra of a water-containing glass. Journal of the American Ceramic Society, 63, 481–485.

Behrens, H., and Yamashita, S. (2008) Water speciation in hydrous sodium tetrasilicate and hexasilicate melts: Constraint from high temperature NIR spectroscopy. Chemical Geology, 256, 306–315.

Bohlen, S.R. (1984) Equilibria for precise pressure calibration and a frictionless furnace assembly for the piston-cylinder apparatus. Neues Jahrbush für Mineralogie-Monatshefte 9, 404–412.

Boyd, F.R., and England, J.L. (1960) Apparatus for phase-equilibrium measurements at pressures up to 50 kilobars and temperatures up to 1750 °C. Journal of Geophysical Research, 65, 741–748.

Davis, K.M., and Tomozawa, M. (1996) An infrared spectroscopic study of water-related species in silica glasses. Journal of Non-Crystalline Solids, 201, 177–198.

Deubener, J., Müller, R., Behrens, H., and Heide, G. (2003) Water and the glass transition temperature of silicate melts. Journal of Non-Crystalline Solids, 330, 268–273.

Efimov, A.M., and Pogareva, V.G. (2006) IR absorption spectra of vitreous silica and silicate glasses: the nature of bands in the 1300 to 5000 cm^{-1} region. Chemical Geology, 229, 198–217.

Eppler, R.A. (1963) Glass formation and recrystallization in the lithium metasilicate region of the system Li_2O-Al_2O_3-SiO_2. Journal of the American Ceramic Society, 46, 97–101.

Holtz, F., Bény, J.M., Mysen, B.O., and Pichavant, M. (1996) High-temperature Raman spectroscopy of silicate and aluminosilicate hydrous glasses: Implications for water speciation. Chemical Geology, 128, 25–39.

Kushiro, I. (1976) A new furnace assembly with a small temperature gradient in solid-media, high-pressure apparatus. Carnegie Institution of Washington Year Book, 75, 832–833.

Le Losq, C., Neuville, D., Moretti, R., and Roux, J. (2012) Determination of water content in silicate glasses using Raman spectrometry: implications for the study of explosive volcanism. American Mineralogist, 97, 779–790.

Le Losq, C., Neuville, D.R., Florian, P., Henderson, G.S., and Massiot, D. (2014) The role of Al^{3+} on rheology and structural changes of sodium silicate and aluminosilicate glasses and melts. Geochimica et Cosmochimica Acta, 126, 495–517.

Le Losq, C., Cody, G.D., and Mysen, B.O. (2015) Alkali influence on the water speciation and the environment of protons in silicate glasses revealed by ^1H MAS NMR spectroscopy. American Mineralogist, 100, 466–473, http://dx.doi.org/10.2138/am-2015-5004.

Malfait, W.J. (2009) The 4500 cm^{-1} infrared absorption band in hydrous aluminosilicate glasses is a combination band of the fundamental {Si,Al}-OH and O-H vibrations. American Mineralogist, 94, 849–852.

Mao, H.K., Bell, P.M., and England, J.L. (1971) Tensional errors and drift of the thermocouple electromotive force in the single stage, piston-cylinder apparatus. Carnegie Institution of Washington Year Book, 70, 281–287.

Moretti, R., Le Losq, C., and Neuville, D.R. (2014) The amphoteric behavior of water in silicate melts from the point of view of their ionic-polymeric constitution. Chemical Geology, 367, 23–33.

Moulson, A.J., and Roberts, J.P. (1961) Water in silica glass. Transactions of the Faraday Society, 57, 1208–1216.

Mysen, B.O. (1990) Role of Al in depolymerized, peralkaline aluminosilicate melts in the systems Li_2O-Al_2O_3-SiO_2, Na_2O-Al_2O_3-SiO_2, and K_2O-Al_2O_3-SiO_2. American Mineralogist, 75, 120–134.

Mysen, B.O., and Cody, G. (2005) Solution mechanisms of H_2O in depolymerozed peralkaline melts. Geochimica et Cosmochimica Acta, 69, 5557–5566.

Mysen, B.O., and Richet, P. (2005) Silicate glasses and melts—Properties and structure. Developments in Geochemistry 10. Elsevier, Amsterdam.

Mysen, B.O., and Virgo, D. (1986) Volatiles in silicate melts at high pressure and temperature 1. Interaction between OH groups and Si^{4+}, Al^{3+}, Ca^{2+}, Na^+ and H^+. Chemical Geology, 57, 303–331.

Mysen, B.O., Finger, L.W., Virgo, D., and Seifert, F.A. (1982) Curve-fitting of Raman spectra of silicate glasses. American Mineralogist, 67, 686–695.

Nakamoto, K., Margoshes, M., and Rundle, R.E. (1955) Stretching frequencies as a function of distances in hydrogen bonds. Journal of the American Chemical Society, 77, 6480–6486.

Novak, A. (1974) Hydrogen bonding in solids. Correlation of spectroscopic and crystallographic data. Structure and Bonding, 18, 177–216.

Nowak, M., and Behrens, H. (1995) The speciation of water in haplogranitic glasses and melts determined by in situ near-infrared spectroscopy. Geochimica et Cosmochimica Acta, 59, 3445–3450.

Schairer, J.F., and Bowen, N.L. (1955) The system K_2O-Al_2O_3-SiO_2. American Journal of Science, 253, 681–746.

——— (1956) The system Na_2O-Al_2O_3-SiO_2. American Journal of Science, 254, 129–195.

Scholtze, H. (1960) Zur Frage der unterscheidung zwischen H_2O-Molekeln und OH-gruppen in gläsern und mineralen. Naturwissenschaften, 47, 226–227.

Spiekermann, G., Steel-McInnis, M., Schmidt, C., and Jahn, S. (2012) Vibrational mode frequencies of silica species in SiO_2-H_2O liquids and glasses from ab initio molecular dynamics. The Journal of Chemical Physics, 136, 154501.

Stolen, R.H., and Walrafen, G.E. (1976) Water and its relation to broken bond defects in fused silica. The Journal of Chemical Physics, 64, 2623–2631.

Stolper, A. (1982) Water in silicate glasses: An infrared spectroscopic study. Contributions to Mineralogy and Petrology, 81, 1–17.

Uchino, T., Sakka, T., and Iwasaki, M. (1991) Interpretation of hydrated states of sodium silicate glasses by Infrared and Raman analysis. Journal of the American Ceramic Society, 74, 306–313.

Wall, T.T., and Hornig, D.F. (1965) Raman intensities of HDO and structure in liquid water. The Journal of Chemical Physics, 43, 2079–2087.

Wu, C.-K. (1980) Nature of incorporated water in hydrated silicate glasses. Journal of the American Ceramic Society, 63, 453–457.

Yamashita, S., Behrens, H., Schmidt, B.C., and Dupree, R. (2008) Water speciation in sodium silicate glasses based on NIR and NMR spectroscopy. Chemical Geology, 256, 231–241.

Zotov, N., and Keppler, H. (1998) The influence of water on the structure of hydrous sodium tetrasilicate glasses. American Mineralogist, 83, 823–834.

Manuscript received June 4, 2014
Manuscript accepted October 29, 2014
Manuscript handled by Grant Henderson